EUROPEAN ORGANIZATION FOR NUCLEAR RESEARCH

CERN-EP/85-19
13 February 1985

INTERMEDIATE-MASS DIMUON EVENTS AT THE CERN $p\bar{p}$ COLLIDER AT $\sqrt{s}$ = 540 GeV

UA1 Collaboration, CERN, Geneva, Switzerland

Aachen[1] - Amsterdam (NIKHEF)[2] - Annecy (LAPP)[3] - Birmingham[4] - CERN[5] - Harvard[6] - Helsinki[7] - Kiel[8] - London (Queen Mary College)[9] - Paris (Coll. de France)[10] - Riverside[11] - Rome[12] - Rutherford Appleton Lab.[13] - Saclay (CEN)[14] - Vienna[15] - Wisconsin[16] Collaboration

G. Arnison[13], O.C. Allkofer[8], A. Astbury[13*], B. Aubert[3], C. Bacci[12], G. Bauer[16], A. Bézaguet[5], R.K. Bock[5], T.J.V. Bowcock[9], M. Calvetti[5], P. Catz[3], P. Cennini[5], S. Centro[+], F. Ceradini[12], G. Ciapetti[12], S. Cittolin[5], D. Cline[16], C. Cochet[14], J. Colas[3], M. Corden[4], D. Dallman[5,15], D. Dau[5,8], M. DeBeer[14], M. Della Negra[3,5], M. Demoulin[5], D. Denegri[14], D. DiBitonto[5], A. Di Ciaccio[12], L. Dobrzynski[10], J.D. Dowell[4], R. Edgecock[4], K. Eggert[1], E. Eisenhandler[9], N. Ellis[5], P. Erhard[1], H. Faissner[1], M. Fincke[8*], P. Flynn[13], G. Fontaine[10], R. Frey[11], R. Frühwirth[15], J. Garvey[4], S. Geer[6], C. Ghesquière[10], P. Ghez[3], K.L. Giboni[1], W.R. Gibson[9], Y. Giraud-Héraud[10], A. Givernaud[14], A. Gonidec[3], G. Grayer[13], W. Guryn[11], T. Hansl-Kozanecka[1], W.J. Haynes[13], L.O. Hertzberger[2], D. Hoffmann[1], H. Hoffmann[5], D.J. Holthuizen[2], R.J. Homer[4], A. Honma[9], W. Jank[5], G. Jorat[5], P.I.P. Kalmus[9], V. Karimäki[7], R. Keeler[9*], I. Kenyon[4], A. Kernan[11], R. Kinnunen[7], W. Kozanecki[11], D. Kryn[5,10], P. Kyberd[9], F. Lacava[12], J.-P. Laugier[14], J.-P. Lees[3], H. Lehmann[1], R. Leuchs[8], A. Lévêque[5], D. Linglin[3], E. Locci[14], M. Loret[14], T. Markiewicz[16], G. Maurin[5], T. McMahon[4], J.-P. Mendiburu[10], M.-N. Minard[3], M. Mohammadi[16], K. Morgan[11], M. Moricca[12], F. Muller[5], A.K. Nandi[9], L. Naumann[5], A. Norton[5], A. Orkin-Lecourtois[10], L. Paoluzi[12], F. Pauss[5], G. Piano Mortari[12], E. Pietarinen[7], M. Pimia[7], D. Pitman[11], A. Placci[5], J.-P. Porte[5], E. Radermacher[1], R. Raja[5], J. Ransdell[11], T. Redelberger[1], H. Reithler[1], J.-P. Revol[5], J. Rich[14], M. Rijssenbeek[5], C. Roberts[13], J. Rohlf[6], P. Rossi[5], C. Rubbia[5,6], B. Sadoulet[5], G. Sajot[10], G. Salvini[12], J. Sass[14], A. Savoy-Navarro[14], D. Schinzel[5], W. Scott[13], T.P. Shah[13], I. Sheer[11], D. Smith[11], J. Strauss[15], J. Streets[4], K. Sumorok[5], F. Szoncso[15], C. Tao[10], G. Thompson[9], J. Timmer[5], E. Tscheslog[1], J. Tuominiemi[7], B. van Eijk[2], J.-P. Vialle[3], J. Vrana[10], V. Vuillemin[5], H.D. Wahl[15], P. Watkins[4], J. Wilson[4], C.-E. Wulz[15], M. Yvert[3] and L. Zanello[12]

(Submitted to Physics Letters B)

*) Now at University of Victoria, Canada.
+ Visitor from the University of Padua, Italy.

ABSTRACT

We report the observation of 21 dimuon events at the CERN $p\bar{p}$ Collider with the UA1 detector. The events range in invariant dimuon mass from 2 to 22 GeV/c^2. The properties of these events are given. The bulk of the events are consistent with heavy-flavour production (mainly $b\bar{b}$) with a few candidates for Drell-Yan production. There remain a few events which are difficult to interpret in terms of these processes, in particular two events with isolated, like-sign muons.

1. INTRODUCTION

We have recently reported five examples of the muonic decay of the neutral Intermediate Vector Boson (IVB) [1]. Since dimuon events have the experimental advantage that the background contamination is small, the search for events with two muons has been extended to the region where both muons have transverse momentum

$$p_T(\mu) > 3 \text{ GeV/c}$$

and

$$|p_T(\mu_1)| + |p_T(\mu_2)| > 10 \text{ GeV/c} \ . \tag{1}$$

In addition to the 5 Z^0 events, 21 events were found (4 like-sign, 17 unlike-sign) with dimuon masses from 2 to 22 GeV/c^2.

There are several expected sources of medium-mass dileptons. The J/ψ and Υ resonances decay into opposite-sign lepton pairs, with muon branching ratios of $\sim$ 7.5% and $\sim$ 3%, respectively. The Drell–Yan mechanism [2]

$$p\bar{p} \to \gamma^* X \to \ell^+ \ell^- X \tag{2}$$

produces opposite-sign leptons with a steeply falling dilepton mass spectrum. Another source is the associated production of heavy quark pairs via the strong interaction of quarks and gluons [3]. The quarks can then decay semileptonically:

$$p\bar{p} \to Q\bar{Q}X \ , \tag{3}$$

$$Q \to q + \ell + \nu \ , \tag{4}$$

where Q = c, b, or t, and q = s, c, or b. Pairs of heavy quarks can also be produced weakly through the decay of IVBs, i.e.

$$p\bar{p} \to W^+ \to t\bar{b} \ , \tag{5}$$

$$p\bar{p} \to Z^0 \to t\bar{t}, b\bar{b}, c\bar{c} \ . \tag{6}$$

In contrast with W and Z production cross-sections, which can be calculated reliably and have been measured in the leptonic decay channels at the CERN $p\bar{p}$ Collider [1, 4, 5], the cross-sections for strong $Q\bar{Q}$ production are subject to various uncertainties. However, once a threshold of $p_T > 3$ GeV/c is applied to the leptons, different predictions [3] agree that the dominant contribution to dileptons is expected to come from $b\bar{b}$ final states rather than $c\bar{c}$. This is due to the hard fragmentation function ($z \sim 0.8$) for b quarks. Whereas process (5) gives like-sign leptons from first-generation decays, processes (3) and (6) yield unlike-sign leptons. However, like-sign dileptons can also originate from process (3) either through second-generation decays ($b \to c \to \mu$) or B^0–$\bar{B}^0$ mixing. Our recent report of a large D^* content in jets [6] suggests that $c\bar{c}$ pair production within the same gluon jet is significant [7]. This mechanism can produce like- and unlike-sign dimuons.

2. DETECTION AND MEASUREMENT OF MUONS, NEUTRINOS, AND JETS

2.1 Muon identification

The UA1 apparatus has already been described elsewhere [8]. The components relevant to the identification and measurement of muons were discussed in detail in ref. [5]. In brief, a muon emerging from the $p\bar{p}$ interaction region traverses the Central Detector (CD), a tracking chamber

that determines the muon momentum by its deflection in the central dipole field of 0.7 T. After leaving the CD, the muon must penetrate the electromagnetic calorimeter, the magnetized hadron calorimeter, and additional iron shielding (typically a total of more than 9 absorption lengths), before reaching the muon chambers. The momentum error due to the measurement errors in the CD is typically $\Delta p/p \sim 0.5\% \times p$ (p in GeV/c). The muon momentum measurements in the final event sample are such that $1/p > 3.5\sigma\,(1/p)$, and thus the charges are unambiguously determined.

2.2 Neutrino identification

The presence of neutrinos is signalled by an apparent transverse-energy imbalance when the calorimeter measurement of missing transverse energy is combined with the muon transverse momentum measurements. For relatively low muon momenta ($p \leq 10$ GeV/c), where the momentum errors on the tracks are small, the accuracy of the missing transverse energy (E_T^{miss}) is $0.7\sqrt{\Sigma E_T}$ GeV, where ΣE_T is the scalar sum of the transverse energy (in GeV) deposited in each calorimeter cell.

2.3 Jet identification

Jets are defined using the standard UA1 jet algorithm [9, 10] applied to energy vectors defined from calorimeter cells. A correction is applied to the measured energy ($\sim +25\%$) and momentum ($\sim +20\%$) of each jet, as a function of the pseudorapidity, azimuth, and transverse energy of the jet, on the basis of test beam data and Monte Carlo studies. The jet energy resolution is typically 18% for a calorimeter jet of $E_T = 15$ GeV, and improves with increasing jet transverse energy. In this paper we consider all jets with $E_T \geq 7.5$ GeV and pseudorapidity $|\eta|$ less than 2.5, keeping in mind, however, that the jet-finding procedure and jet energy measurement become less reliable for $E_T < 15$ GeV.

A jet may be too soft to pass the 7.5 GeV threshold, or sometimes a high-E_T jet is emitted close to the vertical plane where a substantial fraction of the jet energy escapes between adjoining elements of the calorimeters. In either case the charged component of the jet remains well measured, and jet finding is applied to the CD tracks. For the CD jets we impose a threshold of 4.0 GeV/c on the jet p_T (excluding muons), and also $|\eta| < 2.5$. The resulting jet momenta represent only a lower limit to the true value.

In this paper, the jet parameters (for both calorimeter and CD jets) include the muon(s) if the muon(s) is associated with the jet, unless stated otherwise.

3. EVENT SELECTION AND ACCEPTANCE

3.1 Event selection

During the 1983 data-taking period about 2.5×10^6 events were recorded on tape for an integrated luminosity of 108 nb^{-1}. Of these, about 1.0×10^6 events were muon triggers. All the events were passed through a fast filter program, which selected 7.2×10^4 muon candidates with $p_T > 3$ GeV/c. These events were reconstructed by the standard UA1 programs. An automatic selection program, which applied stricter CD track quality and CD/muon chamber matching requirements was used to select dimuon events. Applying the muon p_T cuts (1), 49 candidate dimuon events were selected, and were scanned on a computer graphics display facility. Of these events, 8 were identified as cosmic rays, 4 as 'kinks' (π, K decay) or poor matching between the CD and the muon chamber tracks, and 11 as leakage of hadron showers through cracks in the calorimeters, leaving 26 candidates after scanning.

Five events are Z^0 candidates and have been described in ref. [1]. The muon p_T's of the other 21 events are shown in fig. 1a, along with the p_T cuts applied in the selection.

3.2 Acceptance for muon pairs

We have estimated the acceptance for detecting dimuons from various physical processes using the Monte Carlo method [11, 12]. The muon chambers cover the pseudorapidity range of $|\eta| \lesssim 2.0$, with an average azimuthal acceptance of about 70%; however, the trigger was active for only $|\eta| \lesssim 1.3$. Both muons must be seen in the chambers but only one needs to have triggered. The resulting dimuon acceptance due to the chamber geometry for $b\bar{b}$ and Drell-Yan processes, produced in $|\eta| \lesssim 2.0$, is about 45%. The muon p_T cuts further reduce the acceptance, which is then process-dependent. Because of these p_T cuts, the acceptance for dimuon masses below 10 GeV/c^2 is heavily suppressed and rises rapidly with increasing mass. For masses above $\sim$25 GeV/c^2, there is almost no additional loss from the p_T cut, since the low-p_T muons are also very forward and are cut by the chamber geometry. This acceptance is further reduced by 42% by the CD track quality cuts applied to both muon tracks.

4. BACKGROUND

We have considered a number of possible backgrounds to the muon sample. High-p_T charged hadrons can fake muons either by penetrating the calorimeters and additional iron shielding without interaction, or by leakage of the hadronic shower. These backgrounds have been measured in a test beam and were found to be $\leq 10^{-4}$, after requiring matching between CD and muon chamber tracks. This requirement reduces leakage-induced background to a negligible level. The dominant background is due to pion and kaon decays. The probability for a pion (kaon) to decay in the central region before reaching the calorimeter is $\sim 0.02/p_T$ ($\sim 0.11/p_T$), where p_T is in GeV/c. The background for the dimuon sample has been estimated using all events with one $p_T > 3$ GeV/c muon candidate, and at least one other charged particle with $p_T > 3$ GeV/c. Assuming that pions (kaons) constitute 50% (25%) of all charged particles, we performed a detailed simulation of decays in our detector (including mismeasurements caused by the decays), thereby obtaining a sample of 'fake' dimuon events [13]. Shown in fig. 1a are the absolute numbers of background events integrated over the various regions enclosed by the dashed lines (1.4 events for the total sample). A scan of the 'fake' events shows that most of the background comes from configurations where both muon candidates are in jets. The background for events where both muons are isolated is much lower: for events with both muons having $p_T > 7$ (10) GeV/c the background falls from 0.064 (0.012) events to 0.013 (0.003) events for two isolated muons.

5. GENERAL FEATURES OF THE EVENTS

We first describe the general features of the 21 events which survive the selection criteria (detailed event parameters are in table 1). There are 17 unlike-sign muon pairs and 4 like-sign pairs. The transverse momenta of the individual muons range from the 3 GeV/c cut up to 15 GeV/c (fig. 1a), with a distribution much flatter than expected from background such as $\pi,K \rightarrow \mu$ decays. It is remarkable that the event with the highest transverse muon momentum ($p_T > 10$ GeV/c for both muons) has a like-sign pair.

From the bias due to the muon p_T cuts (1) we expect high-mass pairs (masses above $\sim$ 10 GeV/c^2), with the two muons opposite in azimuth, or low-mass pairs with considerable dimuon transverse momenta. This behaviour is illustrated in fig. 1b, where we show the correlation between the dimuon mass and the opening angle in the transverse plane; fig. 1c shows the correlation between the mass and the p_T of the dimuon system. In most of the events the muons are approximately back-to-back, and in only six events are both muons in the same hemisphere. However, events in the region roughly bounded by

$$[(p_T^{\mu\mu})^2 + (m^{\mu\mu})^2]^{1/2} \lesssim 10\ \text{GeV} \tag{7}$$

are heavily suppressed by the muon p_T cuts (1).

The isolation of the muons is an important tool for distinguishing between the Drell–Yan process and heavy-flavour decays. Muons arising from a process such as the Drell–Yan one should not be embedded in significant hadronic activity, in contrast with c or b quark decays. The overall activity observed in the dimuon events covers a very wide range of transverse energies. Some events have several accompanying jets in the central region, with transverse energies up to 60 GeV/c; others are completely quiet. We classify the muon isolation by calculating the ΣE_T around the muon, i.e. the sum of the transverse energy of all the calorimeter cells within a cone of $\Delta R < 0.7$ about the muon in pseudorapidity (η)–azimuth (ϕ) *) space, where

$$\Delta R = (\Delta\eta^2 + \Delta\phi^2)^{1/2}. \tag{8}$$

The average energy deposition due to the muon itself is subtracted from the sum [10]. The sum ΣE_T for the muons in each event is plotted in fig. 2a, which shows that there is a class of events where both muons are clearly in jets. Taking an isolated muon to be one with $\Sigma E_T < 4$ GeV, we find 9 (3) unlike- (like-) sign events with both muons isolated, 3 (0) events with one isolated muon, and 5 (1) events with neither muon isolated. The dotted curve in fig. 2b is deduced from minimum-bias events in which the ΔR cone was randomly distributed in pseudorapidity and azimuth, and the fluctuations in the energy loss of the muon [10] have been folded into the distribution. It indicates the level of activity present from the underlying event. The dashed curve is a Monte Carlo simulation for $b\bar{b}$ and $c\bar{c}$ production [12]. The heavy-flavour curve is normalized to 9.9 events (according to subsection 6.2), and the minimum-bias curve to 11.1 events, so that the sum of the two curves (solid line) corresponds to 21 events.

Heavy-flavour decays are often accompanied by strange particles. We have searched for K^0's, Λ's, and $\bar{\Lambda}$'s by identifying V^0's. A constrained fit was done on candidate V^0's for each hypothesis (including a γ fit for conversions). A χ^2 cut and a minimum decay length of 0.5 cm were required for consideration. Table 1 contains the results for the hypothesis of the best fit, restricted to the kinematic range $p_T > 0.3$ GeV/c and $|\eta| < 2$. The number of V^0's produced per minimum-bias event for this rapidity range is 0.15 ± 0.04 (0.45 ± 0.09) for $\Lambda/\bar{\Lambda}$ (K) [14].

Heavy-flavour production of dimuons will also yield two neutrinos, which in principle should give rise to missing energy. However, the neutrinos will generally have low p_T because of the bias from the muon p_T cuts. Furthermore, if the neutrinos are back-to-back their transverse momenta will tend to cancel out in the missing E_T . The observed missing energy is, in general, small (see table 1). Because of the poor resolution at small E_T^{miss}, it is not surprising that the average deviation from zero is in fact only 1.4σ.

6. INTERPRETATION

6.1 Drell–Yan production

We have carried out extensive Monte Carlo simulations of Drell–Yan and heavy flavour ($b\bar{b}$ and $c\bar{c}$) production [11, 12]. Drell–Yan events should be characterized by two unlike-sign muons that are isolated, e.g. $\Sigma E_T < 4.0$ GeV in $\Delta R < 0.7$. This isolation criterion is fulfilled for both muons in nine events with unlike-sign pairs. Five of these events (F, G, H, J, X) have the two muons approximately back-to-back in azimuth, with a mass range from 10 GeV/c^2 to 17 GeV/c^2.

*) The azimuthal angle about the beam axis is measured in radians.

The other four events (I, O, M, Z) have the muons in the same hemisphere, and hence with a large $p_T^{\mu\mu}$ (table 1b). In these events the large p_T of the muon pair is balanced by one or more jets. One event (I) is a J/ψ candidate. Note that these four events are well separated from the boundary of the kinematically suppressed region (7). Events from the Drell–Yan Monte Carlo populate a region at lower $p_T^{\mu\mu}$ close to the boundary; however, this depends critically on how steeply the $p_T^{\mu\mu}$ distribution falls at large $p_T^{\mu\mu}$.

Two of the events with back-to-back muons (J, X) are found to have soft jets. The high-$p_T^{\mu\mu}$ events have at least one jet to balance the muons; but two events (M, Z) have more than one jet. Event M is shown schematically in fig. 3.

Assuming that all five events with masses above 10 GeV/c^2 are from Drell–Yan production, we find that the total Drell–Yan cross-section for dimuon masses above 10 GeV/c^2 is 0.6 ± 0.3 nb. This agrees with a recent calculation that yields 0.35 nb for masses above 10 GeV/c^2 [15]. However, we remind the reader that this sample may be contaminated by the Υ resonances as well as by heavy-flavour production (see subsection 6.2), and no correction for this has been applied to the cross-section.

6.2 Production of $b\bar{b}$ and $c\bar{c}$

In another class of events the muons come from heavy-flavour decays and hence are expected to be accompanied by hadronic activity. If we consider the events with at least one non-isolated ($\Sigma E_T > 4$ GeV) muon as being a relatively clean sample of heavy-flavour events, then we have nine such events (fig. 2a). The calculated isolation distribution for $b\bar{b}/c\bar{c}$ production [12] is compared with the data in fig. 2b, the theoretical distribution being normalized relative to the nine non-isolated events. The two distributions are consistent. With this normalization, heavy flavours are estimated to contribute about one event where both muons are isolated. From the Monte Carlo we find that $b\bar{b}$ is the dominant component with our cuts ($c\bar{c}$ contributes ~ 10%), and the cross-section for producing $b\bar{b}$ with both quarks having $p_T > 5$ GeV/c and $|\eta| < 2$ is 2.1 ± 0.8 μb with the above normalization.

There is one like-sign event among the nine non-isolated events. Like-sign events can be produced in the cascade process from $b\bar{b}$, $t\bar{t}$, and $t\bar{b}$ final states, and also from the primary $b\bar{b}$ quarks with B^0–$\bar{B}^0$ mixing. The ratio of like- to unlike-sign events is consistent with the expectations of Monte Carlo simulated $b\bar{b}$ events including the cascade processes, without invoking B^0–$\bar{B}^0$ mixing. Many events have additional high-p_T strange particles (table 1); this favours the heavy-flavour interpretation.

We can form a μ-μ-jet-jet system from the jet associated with each muon, or, when both muons are associated with the same jet, by using the largest opposite jet as the second jet (i.e. jet_1 and jet_2 of table 1)*). The mass of the μ-μ-jet-jet system is shown in fig. 4 , along with QCD calculations (smeared by jet resolution) of heavy flavours, predominantly $b\bar{b}$ [12]. The calculations show a rapidly falling mass distribution, in contrast with a flat distribution for the data. There are three events (R, W, and V) with muons in jets, and a very large mass of the μ-μ-jet-jet system. These events with masses around 100 GeV are compatible with Z^0 decay to heavy flavours, where we expect of the order of one event. These events are characterized by very large additional jet activity. They are less likely to arise from conventional QCD processes, as is also shown in fig. 2b. In particular the like-sign event R is possibly a $Z^0 \rightarrow b\bar{b}$ decay, where one muon comes from a first-generation decay and the other from a second-generation decay (see fig. 5).

*) Event N has no associated jet for one muon; in this case we use the $\Delta R < 0.7$ cone around the muons for the μ-μ-jet-jet system.

6.3 Isolated same-sign events

Three events with like-sign dimuons are observed (Q, S, T) in which both muons are isolated according to our criterion $\Sigma E_T < 4.0$ GeV. In all these events the muon momenta are 6 standard deviations or more from infinite momenta; hence the charges are very well determined. Event T may come from a second-generation decay of a b quark, since one muon is with an identified CD jet. Also one muon p_T is small (the muons are near the kinematical cuts), as would be expected to result from a second-generation decay of a b quark. About one event with two isolated muons is expected from heavy flavours, as discussed in subsection 6.2. Events Q (fig. 6) and S have no jets, and the higher muon p_T's make second-generation $b\bar{b}$ decay unlikely. Both events have a similar topology. In event Q (S) the $\mu^+\mu^+$ ($\mu^-\mu^-$) are back-to-back, and a Λ ($\bar{\Lambda}$) is found at about 90° to both muons in the transverse plane (fig. 6b). In event Q, both muons have very high transverse momenta (larger than 10 GeV); as a consequence the background is small ($< 3 \times 10^{-3}$ events). Calculations have failed to reproduce events with characteristics of event Q from $b\bar{b}$ production with or without B^0–$\bar{B}^0$ mixing. We expect that requiring both muons to have $p_T > 9$ GeV/c will give about 0.2 events with unlike signs and about 0.03 with like signs. We estimate of the order of 10^{-4} events with two isolated like-sign muons. The corresponding rates are about a factor of 10 larger for event S. By invoking mixing, the like-sign rate can be increased by about a factor of 2.

7. SUMMARY

We have observed 21 dimuon events in the mass range 2–22 GeV/c^2. The bulk of these events appear consistent with Drell–Yan or heavy-flavour production. Within the context of the obvious statistical limitations of our event sample, as well as the difficulty of event classification, we find σ_{tot} [$m_{\mu\mu} > 10$ GeV/c^2] ~ 0.6 nb for Drell–Yan, and $\sigma_{tot}[p_T(b,\bar{b}) > 5$ GeV; $|\eta(b,\bar{b})| < 2]$ ~ 2 μb for QCD $b\bar{b}$ production.

In addition, there are three classes of events having characteristics that are not expected from simple Drell–Yan or QCD $b\bar{b}/c\bar{c}$ production. Two of the categories are the isolated, high-p_T dimuons with multijets (M,Z), and the high-mass μ-μ–jet-jet systems of R, V, and W. The third group is composed of isolated like-sign events (Q and S), which are hard to interpret in terms of conventional $b\bar{b}$ production. Event Q is particularly outstanding by virtue of the high muon p_T's.

A complete discussion of dielectron or muon-electron events is not within the scope of this paper; however, we remark that we have found no discrepancies in our dilepton data. Confirmation of the dimuon results in the ee or μe channel is hampered because of the higher p_T cut (typically $p_T > 12$ GeV/c) and the implicit isolation requirements applied to electrons. Fruitful comparison awaits higher statistics.

Acknowledgements

This result has only been made possible by the magnificent performance of the whole CERN Accelerator Group complex. We have received enthusiastic support from H. Schopper and from I. Butterworth for the collider programme.

We are thankful to the management and staff of CERN and of all participating institutes who have vigorously supported the experiment.

The following Funding Agencies have contributed to this programme:

Fonds zur Förderung der Wissenschaftlichen Forschung, Austria.
Valtion luonnontieteellinen toimikunta, Finland.
Institut National de Physique Nucléaire et de Physique des Particules and
Institut de Recherche Fondamentale (CEA), France.
Bundesministerium für Forschung und Technologie, Fed. Rep. Germany.
Istituto Nazionale di Fisica Nucleare, Italy.
Science and Engineering Research Council, United Kingdom.
Department of Energy, USA.

Thanks are also due to the following people who have worked with the Collaboration in the preparation of and data collection on the runs described here: F. Bernasconi, F. Cataneo, R. Del Fabbro, L. Dumps, D. Gregel, J.-J. Malosse, H. Muirhead, G. Salvi, G. Stefanini, R. Wilson, Y.G. Xie and E. Zurfluh.

REFERENCES AND FOOTNOTES

[1] G. Arnison et al. (UA1 Collaboration), Phys. Lett. **147B** (1984) 241.

[2] S.D. Drell and T.M. Yan, Phys. Rev. Lett. **25** (1970) 316.

[3] See for example:
S. Pakvasa et al., Phys. Rev. **D20** (1979) 2862.
F.E. Paige and S.D. Protopopescu, ISAJET program, BNL 29777 (1981).
B.L. Combridge, Nucl. Phys. **B151** (1979) 429.
Z. Kunszt and E. Pietarinen, Nucl. Phys. **B164** (1980) 45.

[4] G. Arnison et al. (UA1 Collaboration), Phys. Lett. **126B** (1983) 398.
G. Arnison et al. (UA1 Collaboration), Phys. Lett. **129B** (1983) 273.
P. Bagnaia et al. (UA2 Collaboration), Phys. Lett. **129B** (1983) 130.
P. Bagnaia et al. (UA2 Collaboration), Z. Phys. **C24,** (1984).
For a review on weak boson production, see E. Radermacher, preprint CERN-EP/84-41 (1984), to be published in Progress in Particle and Nuclear Physics.

[5] G. Arnison et al. (UA1 Collaboration), Phys. Lett. **134B** (1984) 469.

[6] G. Arnison et al. (UA1 Collaboration), Phys. Lett. **147B** (1984) 222.

[7] F. Halzen and F. Herzog, Phys. Rev. **D30** (1984) 2326.

[8] M. Barranco Luque et al., Nucl. Instrum. Methods **176** (1980) 175.
M. Calvetti et al., Nucl. Instrum. Methods **176** (1980) 255.
M. Calvetti et al., IEEE Trans. Nucl. Sci. **NS-30** (1983) 71.
M. Corden et al., Phys. Scr. **25** (1982) 5 and 11.
K. Eggert et al., Nucl. Instrum. Methods **176** (1980) 217.
The UA1 Collaboration is preparing a comprehensive report on the detector, to be published in Nuclear Instrumentation and Methods.

[9] G. Arnison et al. (UA1 Collaboration), Phys. Lett. **132B** (1983) 214. The corrections to jet energies and errors are discussed in 'Correction tables and error estimates for jet energies and momenta', M. Della Negra et al., UA1 Technical Note UA1/TN/84-43 (1984) (unpublished).

[10] A 10 GeV/c muon is expected to deposit about 1.7 GeV in the central calorimeters (at normal incidence). This is an important effect when examining muon isolation or jets with muons. Consequently, the average expected energy deposition is subtracted from the calorimeter cells traversed by the muon. However, for the central hadron calorimeters the energy loss for a 10 GeV/c muon is a Landau distribution peaked at 1.4 GeV and with a r.m.s. of 0.5 GeV (the electromagnetic calorimeters peak at 0.3 GeV, and hence have a small effect). We can then expect that about 2 out of 42 muons will deposit 2 GeV or more in excess of the expected value. This is clearly significant when discussing isolation.

[11] F.E. Paige and S.D. Protopopescu, ISAJET program, BNL 31987 (1982).

[12] These calculations were made using the Eurojet Monte Carlo program which contains all first-order (α_s^2) and second-order (α_s^3) QCD processes [see B. Van Eijk, UA1 Technical Note UA1/TN/84-93 (1984), unpublished, and A. Ali, E. Pietarinen and B. Van Eijk, to be published]. The heavy quark Q is fragmented using the parametrization of C. Peterson et al., Phys. Rev. **D27** (1983) 105, and the V-A decay matrix elements.

[13] G. Bauer et al., UA1 Technical Note UA1/TN/84-21 (1984) (unpublished).

[14] K. Alpgård et al. (UA5 Collaboration), Phys. Lett. **115B** (1982) 65.

[15] G. Altarelli et al., preprint CERN-TH.4015/84 (1984).

Table 1a

Unlike-sign back-to-back dimuons

Event	Muon properties							Jet properties (including muons)				Properties of				Strange particles' properties $p_T > 0.3$ GeV/c, $\|\eta\| < 2.0$				General event properties (including muons)		
												$\mu\mu$		$\mu\mu$-jet$_1$-jet$_2$								
	Q	p_T (GeV/c)	η	ϕ (°)	ΣE_T $\Delta R < 0.7$ (GeV)	μ in jet No.	p_T^{rel} [a] (GeV/c)	Jet No.	p_T (GeV/c)	η	ϕ (°)	Mass (GeV/c^2)	p_T (GeV/c)	Mass (GeV/c^2)	p_T (GeV/c)		p_T (GeV/c)	η	ϕ (°)	E_T^{miss} (GeV)	$\|E_T\|$ (GeV)	E_{tot} (GeV)
F																						
8069	+	5.5 ± 0.3	−1.1	28	0.0							10.2 ± 0.5	1.1 ± 0.3			K^0	0.4	−0.6	122	$1.2^{+2.7}_{-1.2}$	41	366
864	−	4.7 ± 0.3	−1.1	−161	0.8																	
G																						
6782	+	4.4 ± 0.2	0.3	−50	1.0							10.4 ± 0.5	2.6 ± 0.4							3.8 ± 2.3	35	311
154	−	6.1 ± 0.4	0.7	108	1.0																	
H																						
7276	+	4.9 ± 0.4	1.0	−171	0.3							12.1 ± 0.8	2.8 ± 0.7							3.0 ± 1.9	30	186
328	−	7.1 ± 0.6	0.5	27	1.6																	
X																						
8253	+	3.5 ± 0.1	1.2	−61	1.0			1	12.6 ± 4.6	1.0	−125	12.7 ± 1.0	8.1 ± 1.3	40 ± 6	11.5 ± 4.9					5.0 ± 4.1	72	402
986	−	9.5 ± 1.2	−0.1	64	3.9			2[b]	7.9 ± 0.2	1.1	−161											
J																						
6623	+	9.4 ± 1.0	−0.8	−20	1.7			1[b]	5.4 ± 0.1	1.1	98	17.0 ± 1.3	4.5 ± 0.6	44.8 ± 1.8	5.4 ± 0.4	K^0	4.0	1.0	100	$3.4^{+3.5}_{-3.4}$	68	493
333	−	7.9 ± 0.7	−1.2	−171	2.1			2[b]	6.3 ± 0.1	0.7	−96					Λ	1.1	−1.5	−70			
L																						
7051	+	5.8 ± 0.4	0.8	75	1.8	1	1.8 ± 0.1	1[b]	10.6 ± 0.4	0.7	74	12.8 ± 0.8	1.0 ± 0.8	23.0 ± 0.8	0.5 ± 0.7					$2.8^{+3.8}_{-2.8}$	74	420
244	−	6.9 ± 0.7	0.4	−107	5.1	2	1.0 ± 0.1	2[b]	11.0 ± 0.7	0.5	−104			46 ± 7[c]	12.5 ± 4.8[c]							
								3	12.9 ± 4.7	−0.9	126											
P																						
8596	+	9.5 ± 1.1	−0.1	122	2.5	1	1.0 ± 0.2	1[b]	14.1 ± 1.4	−0.1	125	15.1 ± 1.3	4.8 ± 1.4	28.9 ± 1.5	2.5 ± 1.3	K^0	0.9	−0.2	126	5.7 ± 3.9	69	396
1139	−	5.1 ± 0.3	−1.0	−41	6.4	2	2.1 ± 0.2	2[b]	12.1 ± 0.4	−0.8	−49					K^0	1.1	1.9	−160			
N																						
8112	+	6.2 ± 0.2	−1.2	−35	4.3			1	21.9 ± 2.8	−0.6	153	12.4 ± 0.5	0.5 ± 0.5	60 ± 9	$4.3^{+5.2}_{-4.3}$					6.6 ± 4.4	79	446
194	−	5.7 ± 0.3	−0.6	142	13.2	1	1.5 ± 1.0	2	12.1 ± 4.5	1.0	−14											
								3[b]	4.6 ± 0.1	1.1	−91			69 ± 9[c]	$3.0^{+5.2}_{-3.0}$[c]							
Y																						
8316	+	4.8 ± 0.3	−0.6	116	9.4	1	2.3 ± 0.8	1	21.9 ± 2.9	−0.6	138	14.9 ± 2.2	5.1 ± 2.8	60 ± 9	8.2 ± 5.8	K^0	1.2	−1.1	−64	9.6 ± 5.0	97	399
111	−	9.9 ± 2.4	−1.4	−68	11.2	2	2.6 ± 2.7	2	26.6 ± 5.2	−1.4	−58			158 ± 54[c]	10^{+13}_{-10}[c]							
								3	15.9 ± 11.5	2.2	107											
K																						
6894	+	6.3 ± 0.2	1.2	60	12.9	1	3.2 ± 1.0	1	31.0 ± 3.8	1.0	42	18.3 ± 1.0	9.4 ± 1.3	72 ± 10	$5.0^{+6.0}_{-5.0}$					10.7 ± 4.4	87	384
925	−	14.1 ± 1.1	1.4	−153	11.6	2	$2.8^{+3.4}_{-2.8}$	2	29.6 ± 4.4	1.5	−147											
								3[b]	8.2 ± 0.7	−0.1	−14			87 ± 10[c]	6.6 ± 5.9[c]							
V																						
7480	+	6.7 ± 0.8	−1.1	−11	10.0	2	0.2 ± 1.1	1	31.7 ± 4.1	1.2	160	21.9 ± 2.3	2.5 ± 1.0	93 ± 8	12.4 ± 4.9	K^0	0.6	−1.6	−39	$2.9^{+5.2}_{-2.9}$	101	355
1198	−	4.5 ± 0.6	1.5	156	18.7	1	2.0 ± 0.5	2	20.1 ± 2.6	−1.1	−10											
								3	11.5 ± 2.1	0.4	4			207 ± 27[c]	12.5 ± 8.6[c]	$\bar{\Lambda}$	0.4	−1.7	169			
								4	11.1 ± 4.2	−0.8	−167					$\bar{\Lambda}$	1.3	−0.8	78			
								5[b]	4.7 ± 0.1	−0.3	61											
								6	13.9 ± 5.5	−2.5	3											

a) Transverse momentum of μ with respect to the jet axis (with μ removed from jet); b) CD jet; c) Values for the $\mu\mu$ + all jets system.

Table 1b

Unlike-sign same-hemisphere dimuons

Event	Muon properties							Jet properties (including muons)				Properties of $\mu\mu$				Strange particles' properties $p_T > 0.3$ GeV/c, $\|\eta\| < 2.0$				General event properties (including muons)		
	Q	p_T (GeV/c)	η	ϕ (°)	ΣE_T $\Delta R < 0.7$ (GeV)	μ in jet No.	p_T^{rel} [a] (GeV/c)	Jet No.	p_T (GeV/c)	η	ϕ (°)	Mass (GeV/c^2)	p_T (GeV/c)	Properties of $\mu\mu$-jet$_1$-jet$_2$ Mass (GeV/c^2)	p_T (GeV/c)		p_T (GeV/c)	η	ϕ (°)	E_T^{miss} (GeV)	$\|E_T\|$ (GeV)	E_{tot} (GeV)
O																						
8477	+	6.8 ± 0.6	0.0	29	0.3			1[b]	7.6 ± 0.1	−1.1	−103	7.0 ± 0.7	16.7 ± 1.8	30.2 ± 1.8	10.2 ± 1.7	K^0	0.7	0.5	96	8.4 ± 2.6	43	162
95	−	10.9 ± 1.6	0.4	69	0.9											K^0	3.7	−1.1	−102			
I																						
7557	+	12.2 ± 2.4	−0.9	19	3.5			1	16.0 ± 2.9	−2.3	−158	3.1 ± 0.3	15.1 ± 2.7	40 ± 14	$1.1^{+3.6}_{-1.1}$					5.5 ± 3.5	64	453
922	−	3.2 ± 0.1	−0.6	45	3.6																	
M																						
7375	+	9.9 ± 0.7	−1.1	120	0.3			1	22.2 ± 3.4	−0.6	−1	6.8 ± 0.4	15.1 ± 1.0	59 ± 12	3.7 ± 7.6					7.2 ± 3.0	55	205
26	−	6.4 ± 0.6	−0.8	166	1.9			2	11.5 ± 6.4	−1.2	−145											
Z																						
7658	+	3.7 ± 0.2	1.0	152	1.5			1	25.1 ± 4.1	2.4	24	4.8 ± 0.6	15.5 ± 2.8	79 ± 21	19.9 ± 5.5	K^0	0.7	1.9	2	8.8 ± 4.1	81	422
947	−	12.5 ± 2.7	1.0	−167	2.6			2	14.4 ± 2.5	0.5	−31			92 ± 18[c]	22.3 ± 5.5[c]	K^0	0.8	0.5	−39			
								3	4.1 ± 0.1	−0.4	−54											
U																						
7235	+	6.9 ± 0.5	0.5	58	6.1	1	2.8 ± 1.2	1	21.5 ± 2.2	0.6	49	2.0 ± 0.1	10.4 ± 0.7	42.4 ± 4.5	7.2 ± 3.4	K^0	0.9	0.3	−57	4.6 ± 4.2	75	443
798	−	3.7 ± 0.2	0.6	81	3.2	1	2.8 ± 0.5	2	14.8 ± 2.6	0.9	−121			74 ± 43[c]	14 ± 13[c]	Λ	0.4	0.8	−141			
								3	17.1 ± 12.9	2.2	−97											
W																						
8215	+	6.7 ± 0.5	0.6	−129	21.8	1	1.5 ± 1.0	1	36.1 ± 3.8	0.5	−120	2.6 ± 0.2	10.9 ± 0.8	105 ± 13	$5.6^{+9.5}_{-5.6}$	K^0	1.4	−1.2	−138	$0.7^{+7.2}_{-0.7}$	144	494
955	−	4.2 ± 0.2	0.2	−115	21.9	1	1.2 ± 0.3	2	33.4 ± 7.6	−1.4	68											
								3	21.2 ± 3.3	0.8	7			168 ± 15[c]	$8 \pm 8^{+9}_{-8}$[c]	Λ	1.0	−1.2	93			
								4	13.2 ± 2.3	−0.6	−174					$\bar{\Lambda}$	1.4	−0.3	−120			
								5[b]	7.2 ± 0.2	0.0	101											

a) Transverse momentum of μ with respect to the jet axis (with μ removed from jet); b) CD jet; c) Values for the $\mu\mu$ + all jets system.

Table 1c

Like-sign dimuons

Event	Muon properties							Jet properties (including muons)				Properties of				Strange particles' properties $p_T > 0.3$ GeV/c, $\|\eta\| < 2.0$				General event properties (including muons)		
												$\mu\mu$		$\mu\mu$-jet$_1$-jet$_2$								
	Q	p_T (GeV/c)	η	ϕ (°)	ΣE_T $\Delta R < 0.7$ (GeV)	μ in jet No.	p_T^{rel} [a] (GeV/c)	Jet No.	p_T (GeV/c)	η	ϕ (°)	Mass (GeV/c^2)	p_T (GeV/c)	Mass (GeV/c^2)	p_T (GeV/c)		p_T (GeV/c)	η	ϕ (°)	E_T^{miss} (GeV)	$\|E_T\|$ (GeV)	E_{tot} (GeV)
Q																						
8029	+	10.4 ± 1.1	−0.1	28	2.1							21.7 ± 2.3	1.8 ± 1.2			Λ	1.7	−0.5	−66	5.2 ± 3.1	50	254
31	+	11.3 ± 1.4	0.1	−143	2.9																	
S																						
8254	−	5.1 ± 0.2	−0.4	−46	2.6							13.8 ± 0.8	2.4 ± 0.8			$\bar{\Lambda}$	0.7	0.2	45	3.7 ± 3.6	63	458
1179	−	7.3 ± 0.5	0.6	128	1.8																	
T																						
6717	+	3.9 ± 0.1	−1.7	131	2.0			1 [b]	11.7 ± 0.8	−0.1	−75	15.0 ± 0.8	4.0 ± 0.7	18.5 ± 0.7	8.4 ± 0.8	K^0	0.4	−1.5	100	$1.8^{+3.5}_{-1.8}$	60	340
930	+	7.0 ± 0.7	0.2	−77	3.2	1	3.8 ± 0.4															
R																						
8098	−	6.4 ± 0.7	0.5	64	15.8	2	4.1 ± 1.1	1	60.0 ± 6.6	0.4	−151	16.2 ± 2.0	5.5 ± 2.0	107 ± 9	23.7 ± 7.9	K^0	0.4	1.9	81	11.4 ± 6.2	136	433
269	−	10.7 ± 1.6	0.5	−141	40.4	1	2.3 ± 1.9	2	36.6 ± 4.3	0.4	34			135 ± 14 [c]	12.2 ± 9.1 [c]	K^0	1.0	1.7	−112			
								3	11.6 ± 4.4	1.9	21					K^0	1.2	0.6	−101			

a) Transverse momentum of μ with respect to the jet axis (with μ removed from jet); b) CD jet; c) Values for the $\mu\mu$ + all jets system.

Figure captions

Fig. 1 a) The scatter plot of the p_T of the faster muon versus the p_T of the slower muon, with the kinematic boundary of the cuts (solid line). In addition, the number of expected background events integrated over the regions enclosed by the dashed line is indicated (see section 4).
b) The scatter plot of the dimuon mass versus the opening angle between the two muons in the transverse plane .
c) The scatter plot of the dimuon mass versus the dimuon transverse momentum. The positions of the J/ψ and the Υ resonances are indicated for reference.

Fig. 2 The scatter plot (a) shows the transverse energy in a ΔR cone of 0.7 around the fast muon versus the slow muon. The lower plot (b) is the transverse energy in a ΔR cone of 0.7 around each muon [10]. Curves show the distributions for the expectation from $b\bar{b}/c\bar{c}$ production (dashed line) [12], and for a randomly orientated cone in minimum-bias events (dotted line). The sum of the two curves (solid line) corresponds to 42 muons (see text for normalizations).

Fig. 3 Configuration of event M (7375/26) in the plane transverse to the beam axis, and in pseudorapidity (η). Muons are drawn with dashed lines, and jets with solid lines. Jet numbers are those of table 1.

Fig. 4 The mass distribution of the μ-μ-jet-jet system for non-isolated events: a) data, b) Monte Carlo calculation [12] of the expected μ-μ-jet-jet mass distribution from $b\bar{b}$, $c\bar{c} \rightarrow \mu\mu$ production. (Jets are chosen according to subsection 6.2.)

Fig. 5 a) The calorimeter energy flow in ϕ–η space for event R (8098/269). The arrows (length proportional to p_T) indicate the position of the muons.
b) Event configuration for R as in Fig. 3. For this figure the muons are not included in the jet parameters.

Fig. 6 a) The event picture for event Q (8029/31). The two muons are indicated by arrows. Only charged tracks with a $p_T > 0.5$ GeV/c and calorimeter cells with $E_T > 0.5$ GeV are shown.
b) Transverse view of the CD for event Q, showing all charged tracks with $p_T > 0.5$ GeV/c and the π^- track from the Λ^0, which is only 0.2 GeV/c. The sign of the p_T indicates the particle's charge.

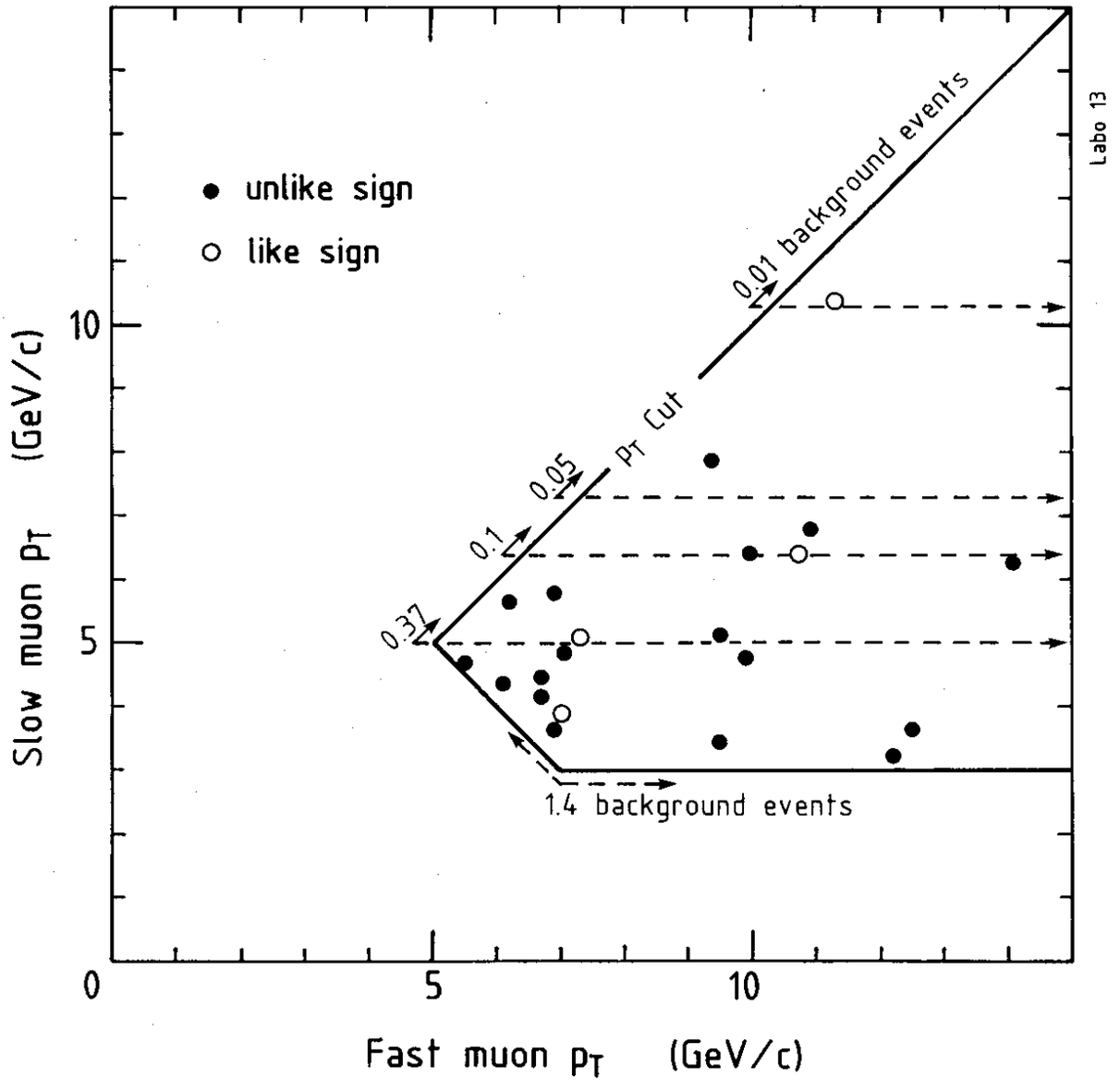
unlike sign
like sign
0.01 background events
p_T Cut
0.05
0.1
0.37
1.4 background events
Slow muon p_T (GeV/c)
Fast muon p_T (GeV/c)
0
5
10
5
10
Labo 13

Fig. 1a

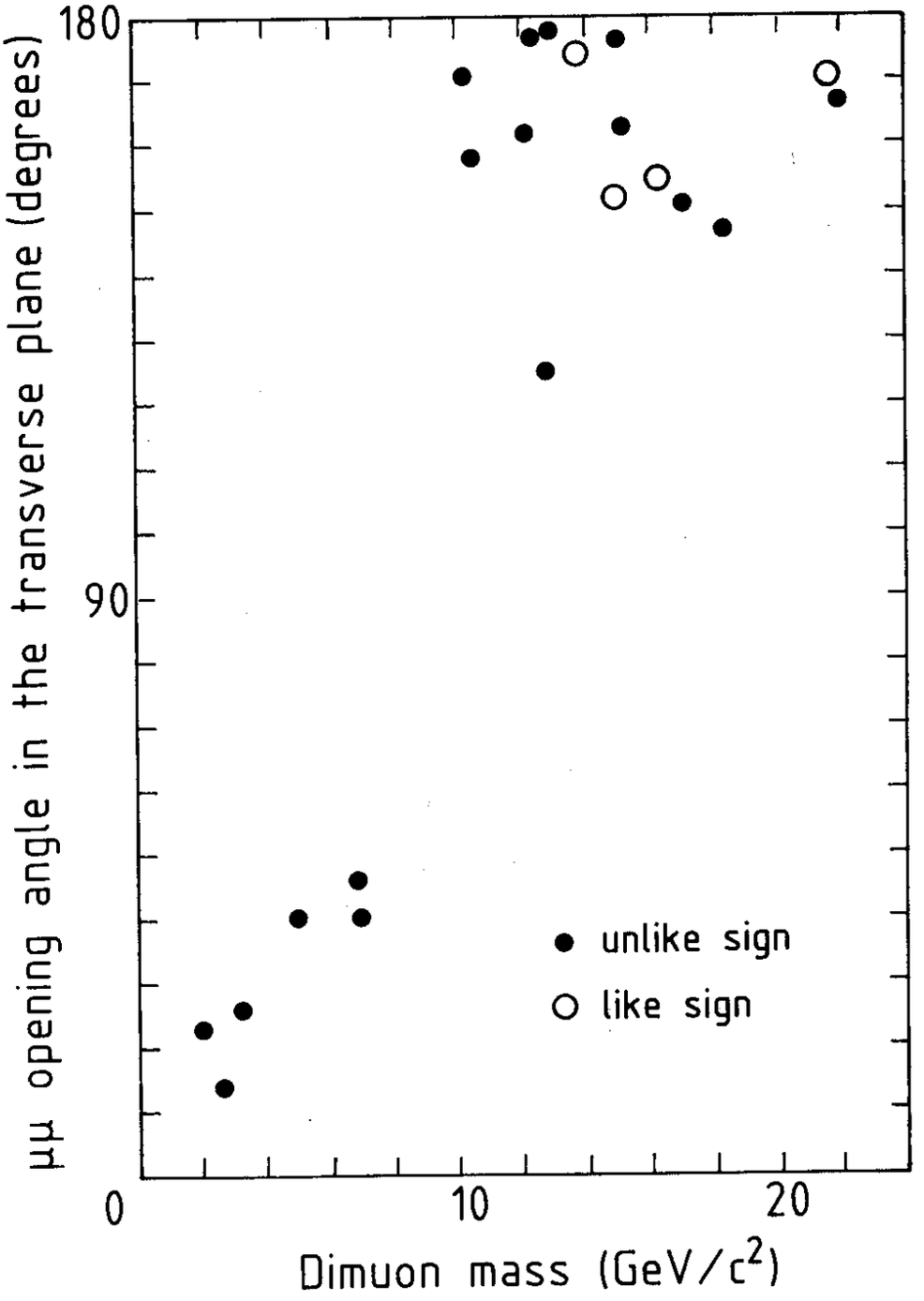
180
90
0
10
20
μμ opening angle in the transverse plane (degrees)
Dimuon mass (GeV/c²)
unlike sign
like sign

Fig. 1b

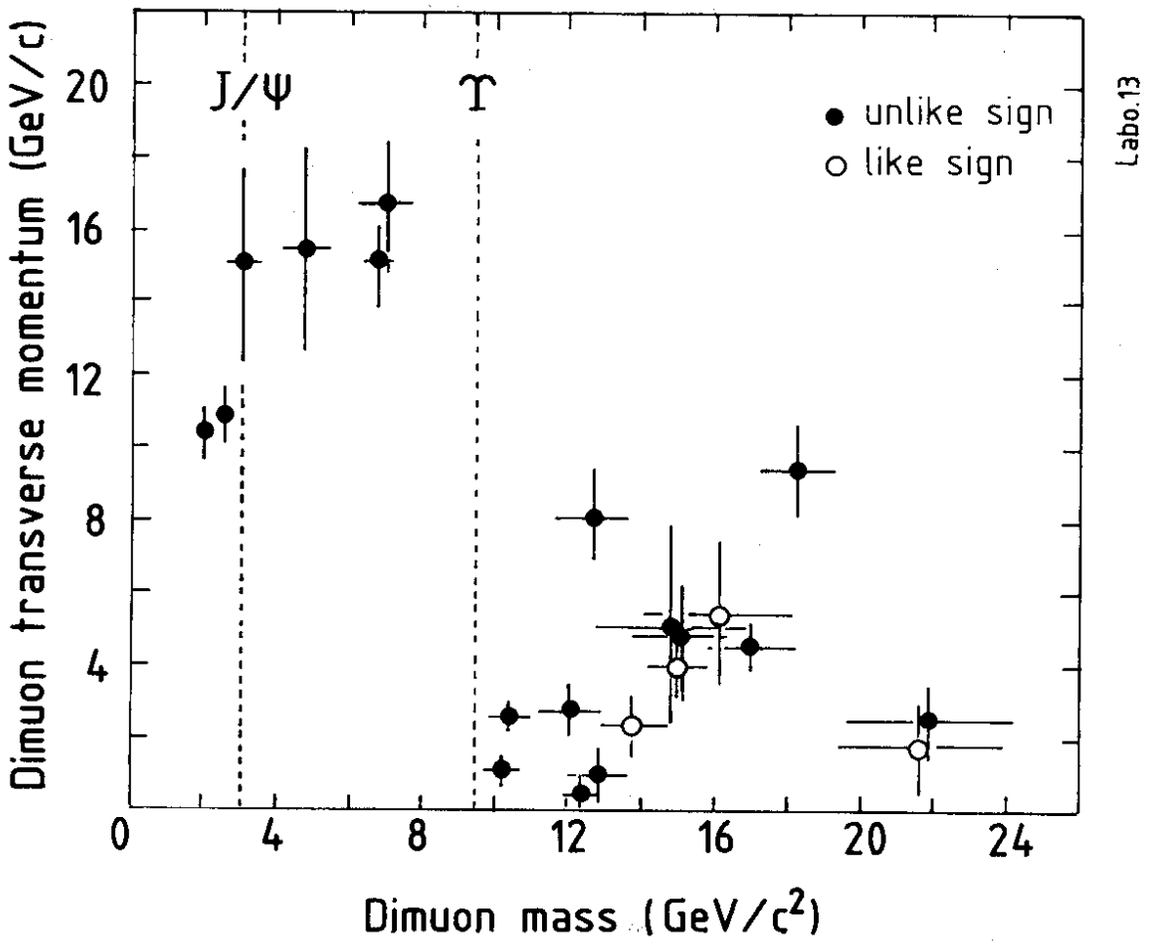
J/Ψ
Υ
● unlike sign
○ like sign
Labo.13
Dimuon transverse momentum (GeV/c)
Dimuon mass (GeV/c²)
0
4
8
12
16
20
24

Fig. 1c

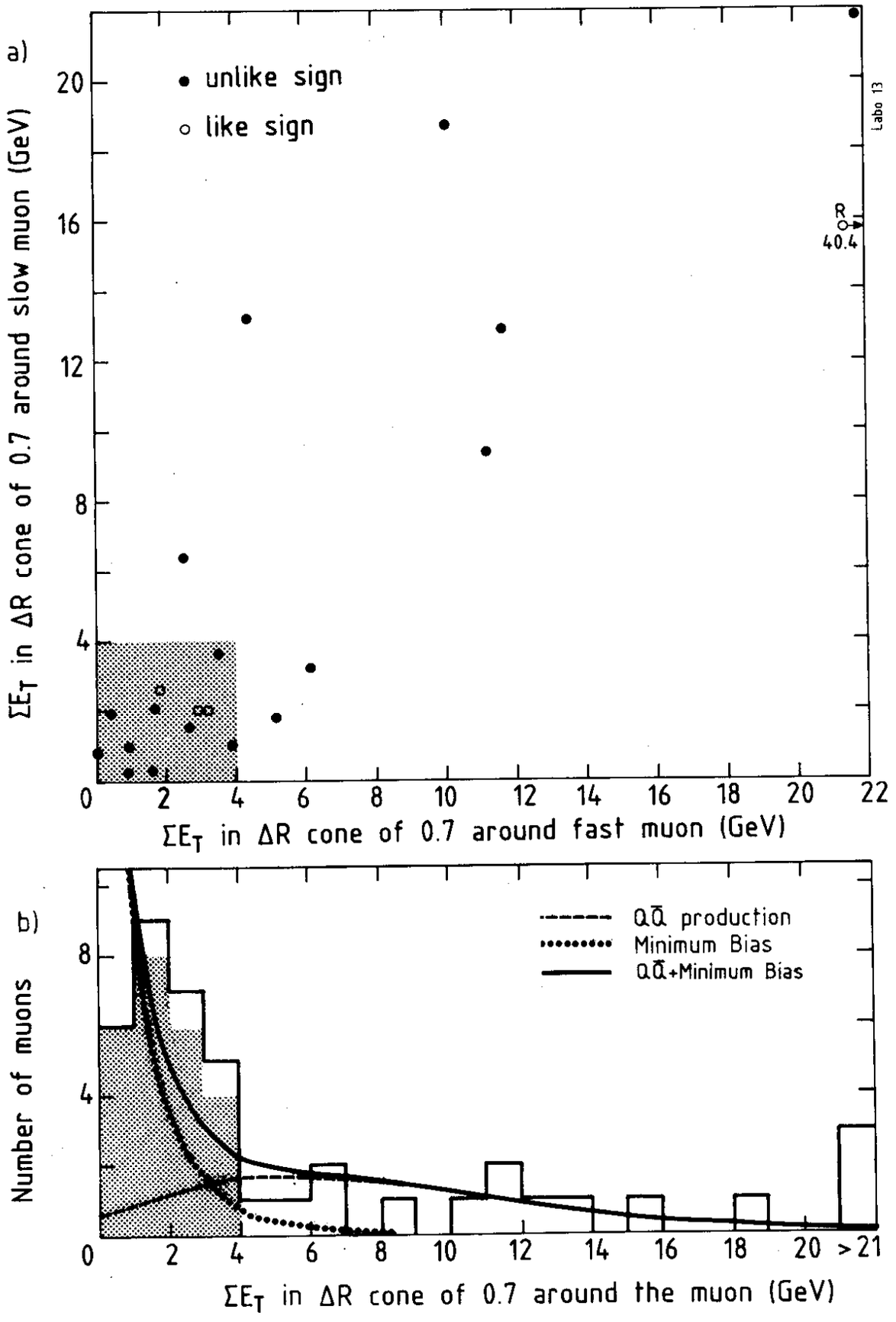
a)
unlike sign
like sign
Labo 13
R
40.4
ΣE_T in ΔR cone of 0.7 around slow muon (GeV)
ΣE_T in ΔR cone of 0.7 around fast muon (GeV)
b)
$Q\bar{Q}$ production
Minimum Bias
$Q\bar{Q}$+Minimum Bias
Number of muons
ΣE_T in ΔR cone of 0.7 around the muon (GeV)

Fig. 2

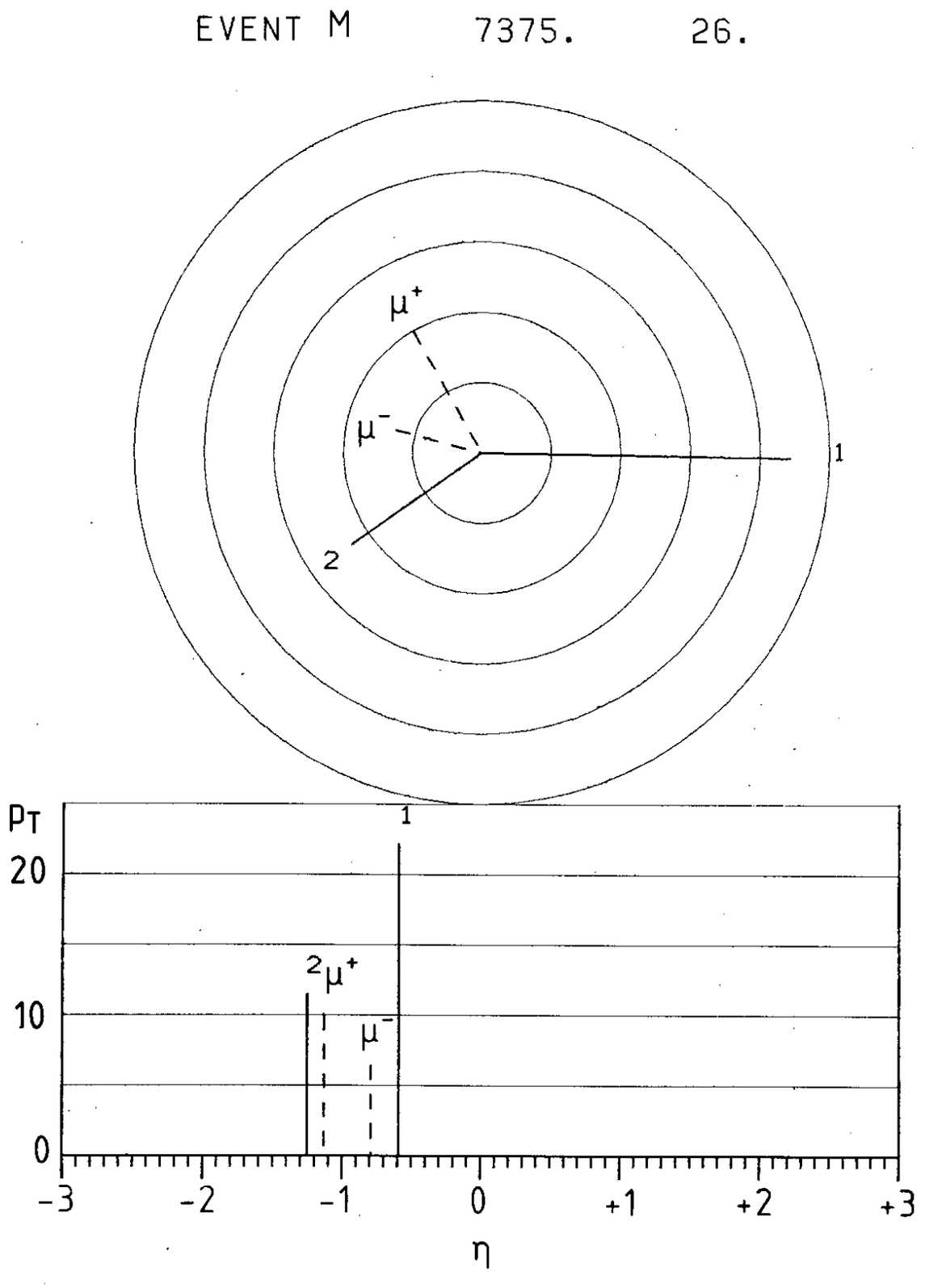

Fig. 3

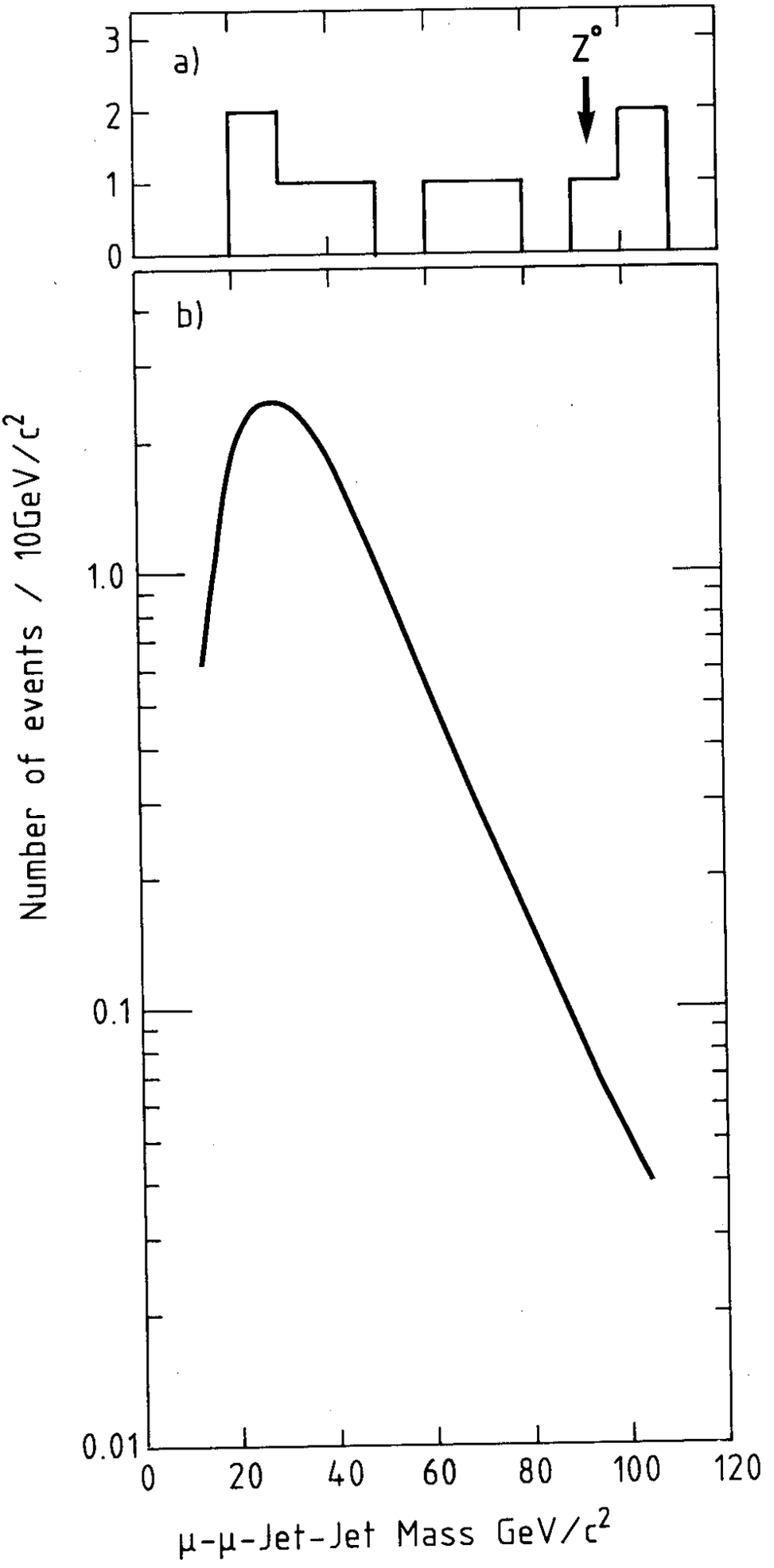
a)
Z°
3
2
1
0
b)
1.0
0.1
0.01
Number of events / 10GeV/c²
0
20
40
60
80
100
120
μ-μ-Jet-Jet Mass GeV/c²

Fig. 4

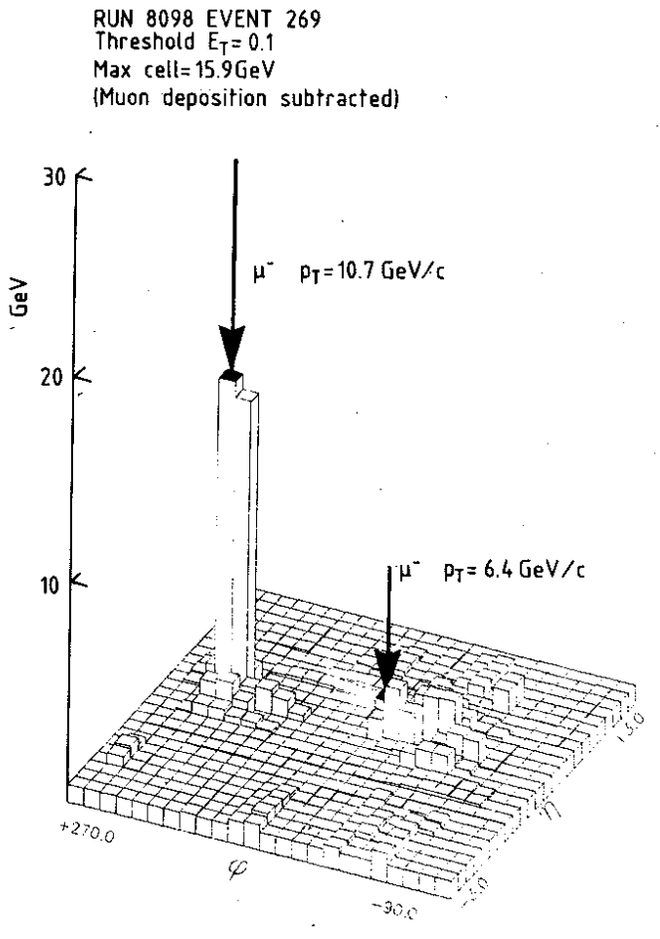
RUN 8098 EVENT 269
Threshold E_T = 0.1
Max cell = 15.9 GeV
(Muon deposition subtracted)
GeV
30
20
10
μ⁻ p_T = 10.7 GeV/c
μ⁻ p_T = 6.4 GeV/c
+270.0
φ
-90.0

a)

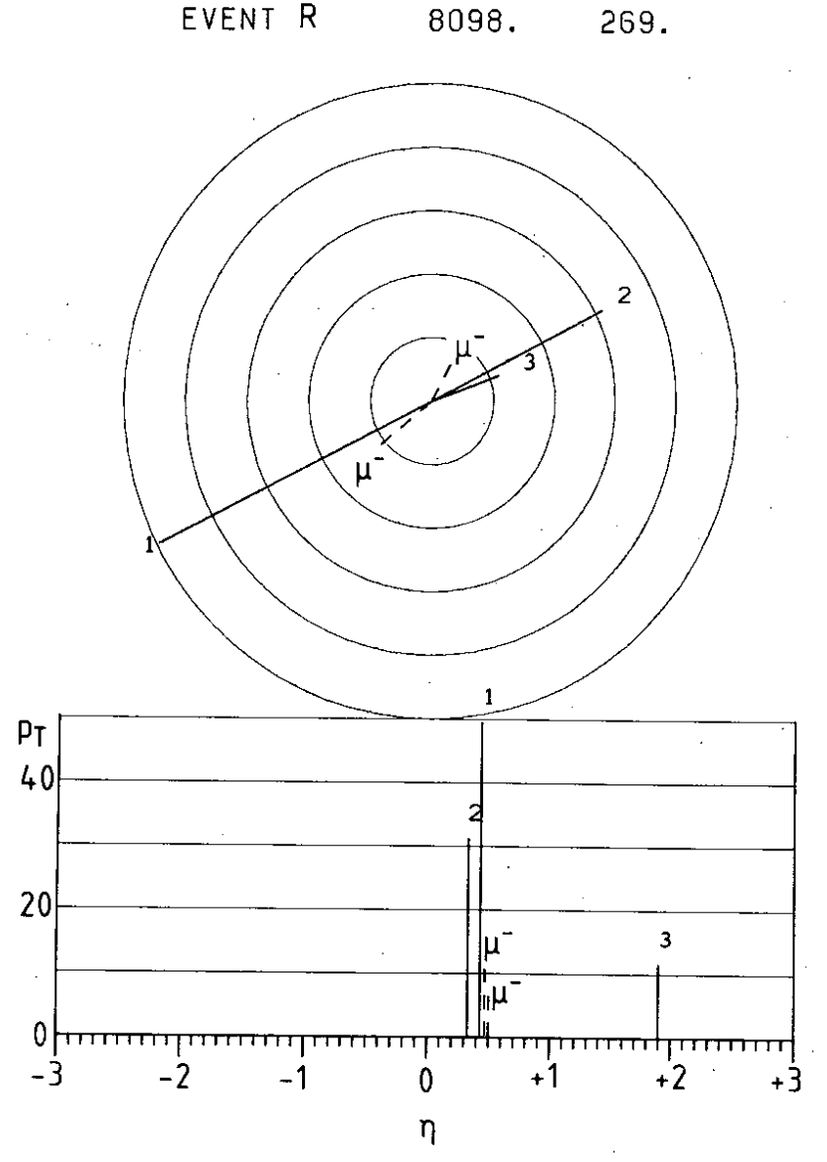
EVENT R 8098. 269.
μ⁻
μ⁻
1
2
3
1
P_T
40
20
0
2
3
μ⁻
μ⁻
-3
-2
-1
0
+1
+2
+3
η

b)

Fig. 5

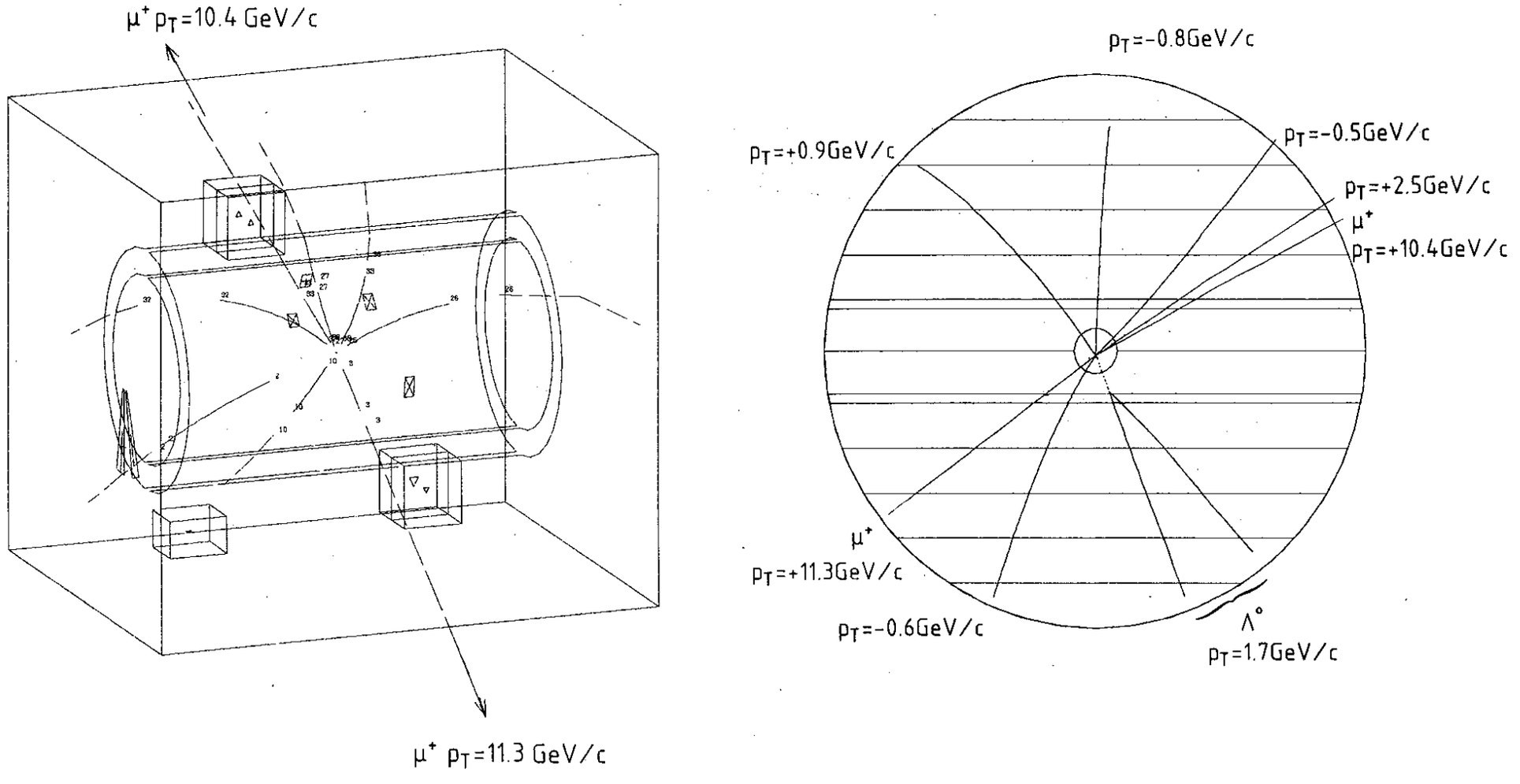
RUN 8029 EVENT 31
Threshold p_T=0.5 E_T=0.5
μ^+ p_T=10.4 GeV/c
μ^+ p_T=11.3 GeV/c
a)
p_T=-0.8GeV/c
p_T=+0.9GeV/c
p_T=-0.5GeV/c
p_T=+2.5GeV/c
μ^+
p_T=+10.4GeV/c
μ^+
p_T=+11.3GeV/c
p_T=-0.6GeV/c
Λ°
p_T=1.7GeV/c
b)

Fig. 6